Time-resolved photoluminescence study of InGaAs/GaAs quantum wells on (111)B GaAs substrates under magnetic fields

F. Y. Tsai, C. P. Lee, O. Voskoboynikov, H. H. Cheng, Jinxi Shen, and Yasuo Oka

Articles you may be interested in

Confirmation of the pyroelectric coefficient of strained In x Ga 1x As/GaAs quantum well structures grown on (111)B GaAs by differential photocurrent spectroscopy
J. Appl. Phys. **91**, 3002 (2002); 10.1063/1.1445278

Determination of the pyroelectric coefficient in strained InGaAs/GaAs quantum wells grown on (111)B GaAs substrates
J. Appl. Phys. **90**, 915 (2001); 10.1063/1.1379563

Effects of the piezoelectric field on quantum-confined Stark effect in (111)B InGaAs quantum-well structure
J. Appl. Phys. **85**, 2221 (1999); 10.1063/1.369530

Barrier thickness dependence of the photoscreening of the piezoelectric field in (111) orientated GaAs–In x Ga 1x As double quantum wells
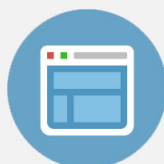J. Appl. Phys. **84**, 3349 (1998); 10.1063/1.368491

Characterization of piezoelectric (111)B InGaAs/GaAs p-i-n quantum well structures using photoreflectance spectroscopy
Appl. Phys. Lett. **72**, 1208 (1998); 10.1063/1.121015

Time-resolved photoluminescence study of InGaAs/GaAs quantum wells on (111)*B* GaAs substrates under magnetic fields

F. Y. Tsai, C. P. Lee,[a)] and O. Voskoboynikov
Department of Electronic Engineering, National Chiao Tung University, Hsin Chu, Taiwan

H. H. Cheng
Condensed Matter Center, National Taiwan University, Taipei, Taiwan

Jinxi Shen and Yasuo Oka
Research Institute for Scientific Measurements, Tohoku University, Katahira, Sendai, Japan

The exciton dynamics in $In_xGa_{1-x}As/GaAs$ quantum wells grown on (111)*B* and (100) GaAs substrates were studied by time-resolved photoluminescence (PL) under magnetic fields in a Faraday configuration. We have found that the piezoelectric fields in (111)*B* samples affect the transient behavior of the PL spectra. Compared with the reference (100) sample, we have found that the strong piezoelectric fields, as well as the magnetic fields, cause a slower spin–flip process in (111)*B* strained quantum wells. © *2001 American Institute of Physics.*
[DOI: 10.1063/1.1376401]

I. INTRODUCTION

Epitaxial layers grown on III–V substrates with (111) orientation possess many interesting properties and have therefore attracted a lot of attention recently. When there is strain in the layers, a strong internal field is induced because of the piezoelectric effect.[1] A lot of effort has been devoted to the growth of strained quantum wells and the study of the piezoelectric effect.[2–5] However, studies on the exciton relaxation of the strained quantum wells under strong piezoelectric fields are very limited,[6,7] although there has been a lot of work on the exciton dynamics of quantum wells.[8–13] In this work, time-resolved photoluminescence (PL) is used to study the exciton dynamics of InGaAs/GaAs quantum wells on (111)*B* GaAs substrates under magnetic fields. Compared with the result obtained from samples grown on (100) substrates, we found unique dynamic behavior in (111)*B* InGaAs/GaAs quantum wells. The phenomenon is related to the spin–flip process under strong piezoelectric fields.

II. EXPERIMENT

The samples, which had a single 1.5 nm $In_xGa_{1-x}As/GaAs$ quantum well with a 50 nm GaAs cap layer, were grown by molecular beam epitaxy. The layers were grown on both (111)*B* and (100) GaAs substrates which were placed side by side in the chamber for comparison. The GaAs layers were grown at 590 °C and the InGaAs layers were grown at 520 °C. For the time-resolved PL measurement, the samples were excited by an amplified mode-locked titanium–sapphire laser and an optical parametric amplifier (OPA) system from Spectra Physics with a laser energy at 3.1 eV. The time-resolved PL spectra were measured by a Hamamatsu streak camera (C4334) with a time

resolution of 5 ps. The measurements were performed at 4.2 K. Magnetic fields up to 6 T were applied in a Faraday configuration during the measurements.

III. RESULTS AND DISCUSSION

In our measurement, the PL intensity was obtained in both the time domain and the wavelength domain. When the data are integrated over the time domain, ordinary PL spectra are obtained. On the other hand, if the data are integrated over the wavelength domain, time-resolved curves are obtained. Figure 1 shows the emission spectra of a InGaAs quantum well grown on the (111)*B* substrate at different magnetic fields. The In composition was 25%. The linewidths of all peaks shown in Fig. 1 are less than 3 meV, indicating excellent material quality. The diamagnetic shift towards higher energy is evident as the magnetic field is increased. Diamagnetic shifts of samples grown on different substrates and with different. In compositions in the quantum wells are shown in Fig. 2. The energy of the shift for the quantum wells grown on the (111)*B* substrate is much larger than that of the quantum wells grown on the (100) substrate. This is because of the reduced exciton binding energy in the (111)*B* quantum wells caused by the strong piezoelectric field, which reduces the Coulomb interaction between the electron and the hole inside the exciton. The results of samples with an In composition of 25% in the (111)*B* and (100) directions are consistent with our previous work in continuous wave (cw) PL measurements.[14] We noticed that, in Fig. 1, the emission intensity increases with magnetic field. At a magnetic field of 6 T, the peak intensity increases by about 30% compared with that without a magnetic field. This is because the magnetic field confines the electron and hole wave functions in the lateral directions and increases the probability of exciton formation.

Figure 3 shows the measured time-resolved curves of a (111)*B* InGaAs quantum well with an In composition of

---
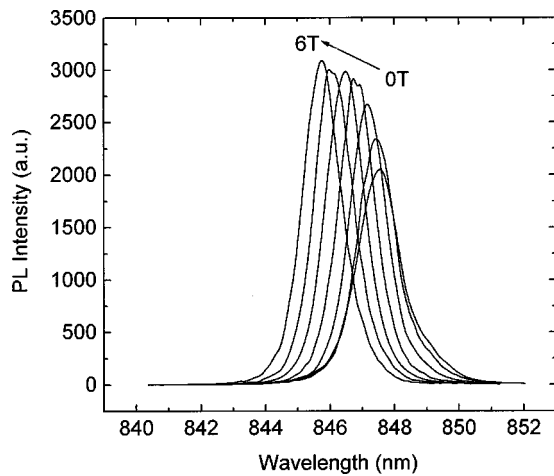[a)]Electronic mail: cplee@cc.nctu.edu.tw

FIG. 1. Photoluminescence spectra of a (111)B In$_{0.25}$Ga$_{0.75}$As/GaAs1.5 nm quantum well under various magnetic fields.

FIG. 3. Time-resolved PL curves of a (111)B In$_{0.25}$Ga$_{0.75}$As/GaAs 1.5 nm quantum well with and without a magnetic field of 6 T. The solid lines show the fitting results by including the spin–flip process using Eq. (1).

25%. The two curves correspond to results with and without a magnetic field of 6 T. In this semilog plot, we can see clearly that the curves cannot be fitted by a single decay time constant of radiative recombination. Instead, we can fit the curves very well using two time constants for the decay part. The equation used for fitting is

$$I(t) = I_0(a e^{-(t/\tau_1)} + b e^{-(t/\tau_2)} - c e^{-(t/\tau_0)}), \qquad (1)$$

where

$$a + b = c. \qquad (2)$$

The rise time is governed by τ_0, but the fall time is governed by τ_1 and τ_2. The fitted curves shown in Fig. 3 agree very well with the measured data.

It is common to attribute the two-exponential behavior of the PL decay curves in quantum wells to localized exciton states induced by interface roughness. However, this is not the case here. Because of the narrow well widths used in our samples, a small variation of the width will cause a large shift in the exciton energy. As a result, it will widen the PL linewidth significantly. While in our PL spectra, whether they were excited in pulse mode or cw mode, the linewidths
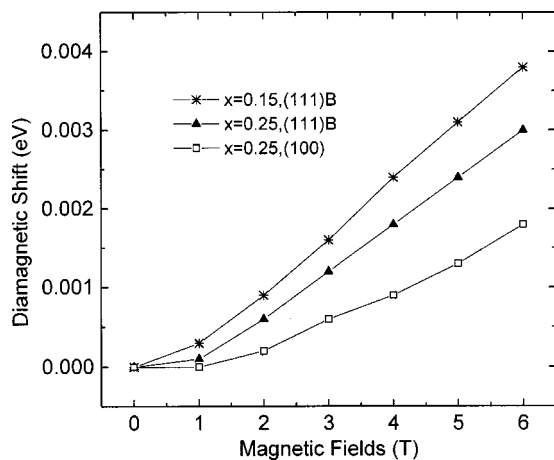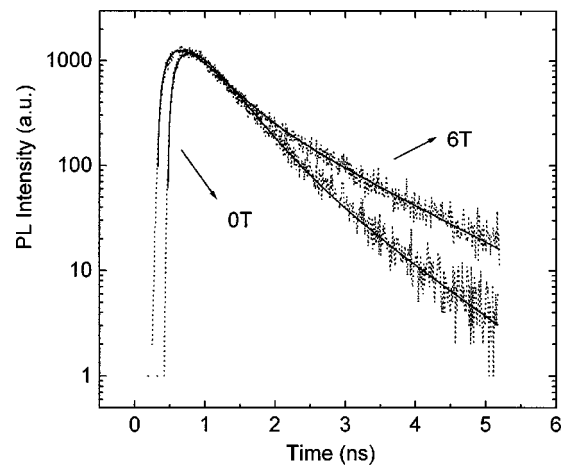
of all the samples are below 3 meV. Therefore, the interface roughness in our samples should be minimal.

The spin–flip mechanism is considered to be the reason for the two-exponential behavior of the decay curves. For electrons with angular momentum $+\frac{1}{2}$ or $-\frac{1}{2}$, and heavy holes with $+\frac{3}{2}$ or $-\frac{3}{2}$, radiative recombination happens only for excitons with combinations of $(+\frac{1}{2}, +\frac{3}{2})$ and $(-\frac{1}{2}, -\frac{3}{2})$, the so-called bright excitons. For $(-\frac{1}{2}, +\frac{3}{2})$ and $(+\frac{1}{2}, -\frac{3}{2})$ combinations, the dark excitons, radiative recombination is forbidden. Except for nonradiative recombination, the only way for carriers to relax from the dark exciton levels is the spin–flip process. In this process, the electron or the hole in the dark exciton changes its spin to become a bright exciton so that radiative recombination is possible. A schematic of this is shown in Fig. 4. Let $\tilde{N}_0$ be the number of electron-hole pairs excited by the incident laser source. τ_{0d} is the time constant for the relaxation from the excited level to the dark exciton level and τ_{0b} is the time constant for the exciton to relax to the bright exciton level. τ_{db} is the time constant for spin flip from the dark exciton level to the bright exciton level. τ_{bd} is the time constant for spin flip from the bright exciton level to the dark exciton level. τ is the radiative recombination time constant of bright excitons. τ_{dn} is the nonradiative recombination time constant of dark excitons. τ_{bn} is the nonradiative recombination time constant of bright excitons. n_0 is the number of excitons at the excited level. n_d
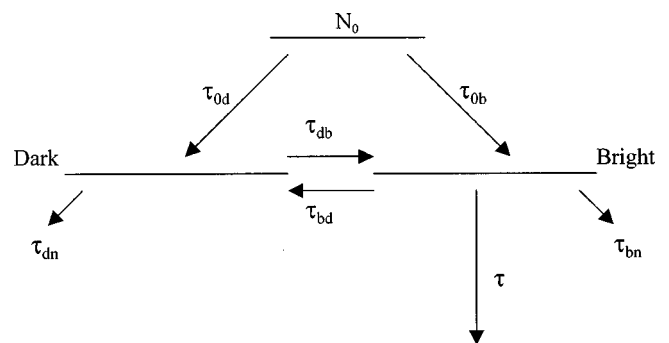

FIG. 2. Diamagnetic shifts of the PL peak energy under magnetic fields in a Faraday configuration.

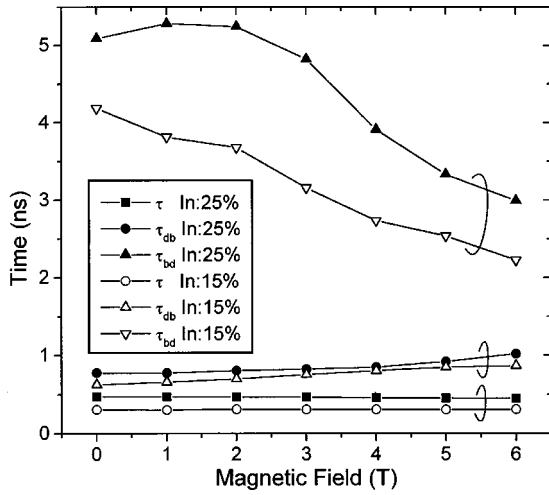FIG. 4. Schematic of the exciton relaxation.

FIG. 5. Radiative recombination time constant τ, the spin–flip time constant τ_{db}, and τ_{bd} as functions of the magnetic field.

is the number of excitons at the dark exciton level. n_b is the number of excitons at the bright exciton level. The rate equations that govern their populations are

$$\frac{dn_0}{dt} = -\frac{n_0}{\tau_0}, \quad \frac{1}{\tau_0} = \frac{1}{\tau_{0d}} + \frac{1}{\tau_{0b}}, \tag{3}$$

$$\frac{dn_d}{dt} = -\frac{n_d}{\tau_d} + \frac{n_b}{\tau_{bd}} + \frac{n_0}{\tau_{0d}}, \quad \frac{1}{\tau_d} = \frac{1}{\tau_{db}} + \frac{1}{\tau_{dn}}, \tag{4}$$

and

$$\frac{dn_b}{dt} = -\frac{n_b}{\tau_b} + \frac{n_d}{\tau_{db}} + \frac{n_0}{\tau_{0b}}, \quad \frac{1}{\tau_b} = \frac{1}{\tau_{bd}} + \frac{1}{\tau_{bn}}\frac{1}{\tau}, \tag{5}$$

with initial conditions $n_0(0) = \tilde{N}_0$, $n_d(0) = 0$, and $n_b(0) = 0$. By solving Eqs. (3)–(5) with the nonradiative terms $1/\tau_{dn}$ and $1/\tau_{bn}$ neglected, we get

$$n_b(t) = \tilde{N}_0 \Bigg[A\left(\frac{1}{\tau_{db}\tau_0} - \frac{1}{\tau_{0b}\tau_1} \right) e^{(t/\tau_1)}$$

$$+ B\left(\frac{1}{\tau_{db}\tau_0} - \frac{1}{\tau_{0b}\tau_2} \right) e^{(t/\tau_2)}$$

$$+ C\left(\frac{1}{\tau_{db}\tau_0} - \frac{1}{\tau_{0b}\tau_0} \right) e^{(t/\tau_0)} \Bigg], \tag{6}$$

where

$$A = \frac{\tau_1(\tau_2 - \tau_0)}{\tau_0(\tau_1 - \tau_2)} C, \tag{7}$$

$$B = \frac{\tau_2(\tau_0 - \tau_1)}{\tau_0(\tau_1 - \tau_2)} C, \tag{8}$$

$$\frac{1}{C} = \frac{1}{\tau_0^2} - \frac{1}{\tau_0}\left(\frac{1}{\tau_1} + \frac{1}{\tau_2} \right) + \frac{1}{\tau_1 \tau_2}, \tag{9}$$
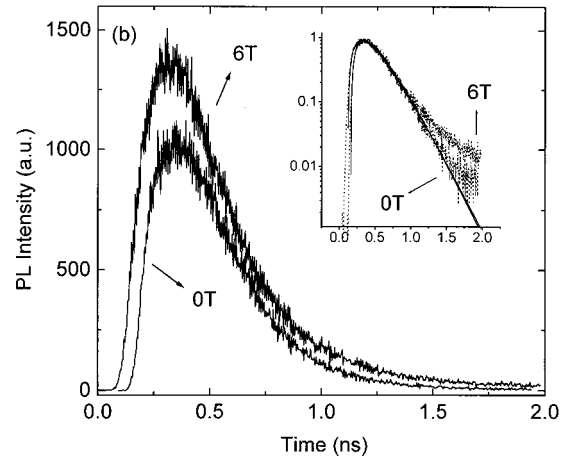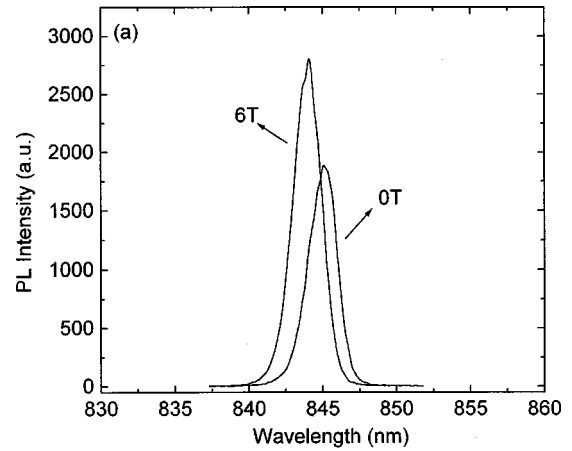

FIG. 6. Comparison of the peak intensity changes with or without the magnetic field, (a) in the time integrated PL spectra and (b) in the time evolution of the PL peak for a (100) $In_{0.25}Ga_{0.75}As/GaAs$ 1.5 nm quantum well. The inset shows the normalized curves (dotted lines) on a semilog scale and the fitted results (solid lines).

$$\frac{1}{\tau_1} = \frac{1}{2}\left[\left(\frac{1}{\tau_b} + \frac{1}{\tau_d} \right) - \sqrt{ \left(\frac{1}{\tau_b} + \frac{1}{\tau_d} \right)^2 - \frac{4}{\tau_{db}\tau} } \right], \tag{10}$$

$$\frac{1}{\tau_2} = \frac{1}{2}\left[\left(\frac{1}{\tau_b} + \frac{1}{\tau_d} \right) + \sqrt{ \left(\frac{1}{\tau_b} + \frac{1}{\tau_d} \right)^2 - \frac{4}{\tau_{db}\tau} } \right]. \tag{11}$$

By fitting Eq. (6), which is basically the same as Eq. (1), to the measured time-resolved PL, we can obtain the various time constants. The fitted results for (111)B samples are shown in Fig. 5. In all samples, τ is almost the same, while τ_{bd} is larger than τ_{db} in all magnetic fields, meaning that the bright exciton energy level is lower than the dark exciton energy level. Meanwhile, as the magnetic field increases, τ_{bd} decreases and τ_{db} increases, which means the bright exciton energy level goes upward and the dark exciton energy level goes downward with the increase of the magnetic field.

For the (100) quantum wells, the time-resolved luminescence curve, shown in Fig. 6, is quite different. The exponential decay of the light intensity comes mostly from the short time constant. The contribution from the longer decay time constant is negligible. As shown in the inset of Fig. 6(b), the decay curve (dotted lines) does not deviate from the fitted exponential curves (solid lines) until the intensity is

less than 5% of the peak intensity, even under 6 T magnetic field. So, it is reasonable to fit the time-resolved curves using a single exponential decay term, which is the radiative time constant. The time constant is around 180 ps for all magnetic fields. From a comparison of the measured results of samples in the (111)B and (100) orientations, it can be concluded that the separation of the bright and dark exciton levels might be due to the strong piezoelectric field induced by the strain in (111)B samples. Also shown in Fig. 5, τ_{bd} is larger when the In composition is higher for the (111)B sample while τ_{db} is comparable in both cases, meaning the separation is larger for higher In concentration. This again is caused by the stronger piezoelectric field induced by higher strain. Further theoretical calculations are needed to study the effect of the piezoelectric fields on the spin dynamics in strained quantum structures.

There is also a difference in the exciton population between (111)B and (100) samples. When the high-energy photons of the laser pulse hit the sample, only hot bright excitons are created according to the selection rule. The hot excitons cool down quickly by releasing phonons. Some of those phonons might induce the dissociation of other excitons. Then the dissociated carriers might combine again to form excitons. During this cooling process, the number of dark excitons increases. Because of the low binding energy for excitons in (111)B samples due to strong piezoelectric fields, there are more carriers at the dark exciton level. As the magnetic fields increase, τ_{bd} decreases and τ_{db} increases. The number of excitons at the dark exciton level also increases. From the time-resolved curves shown in Fig. 3, we can compare the relative bright exciton populations at different magnetic fields by comparing the peak intensity of each curve. Since the peak intensity is almost the same under different magnetic fields, the initial bright exciton population is about the same and is independent of the magnetic field. However, in Fig. 1, which shows the time integrated PL spectra, we found that the PL peak intensity increases with the magnetic field. So, although the initial bright exciton population is the same, the total exciton emission is higher for higher magnetic field. This is because the number of dark excitons increases with the magnetic field and these dark excitons switch to bright excitons with a time constant τ_{db} through the spin–flip process and τ_{db} gets longer for a stronger magnetic field. The dark exciton to bright exciton ratio is quite different for the (100) sample. Figure 6 shows the PL spectra and the time-resolved curves of this sample. The ratio

in peak intensity with and without a magnetic field (6 T) is about the same for both the integrated PL spectrum and the time-resolved curve. The decay time constant is also about the same with and without the magnetic field. So, the contribution from the dark excitons is very small. It is a good approximation to neglect the dark exciton effect in the (100) sample and the result is reproducible in other (100) samples.

IV. CONCLUSIONS

We have studied time-resolved photoluminescence of In$_x$Ga$_{1-x}$As/GaAs quantum wells grown on (111)B and (100) substrates. Magnetic fields up to 6 T in a Faraday configuration were used during the measurements. The spin–flip process was found to play an important role in the exciton relaxation in (111)B strained quantum wells because of the strong piezoelectric fields. The spin–flip time from the dark exciton level to the bright exciton level increases with the magnetic field. Further theoretical calculations are needed to evaluate this phenomenon.

ACKNOWLEDGMENT

[1] C. Mailhiot and D. L. Smith, Phys. Rev. B **35**, 1242 (1987).
[2] J. M. Ballingall and C. E. C. Wood, Appl. Phys. Lett. **41**, 947 (1982).
[3] A. S. Pabla, J. Woodhead, E. A. Khoo, R. Grey, J. P. R. David, and G. J. Rees, Appl. Phys. Lett. **68**, 1595 (1996).
[4] I. H. Campbell, D. E. Watkins, D. L. Smith, S. Subbanna, and H. Kroemer, Appl. Phys. Lett. **59**, 1711 (1991).
[5] E. S. Snow, B. V. Shanabrook, and D. Gammaon, Appl. Phys. Lett. **56**, 758 (1990).
[6] C. H. Molloy, X. Chen, D. A. Woolf, D. J. Somerford, and P. Blood, CLEO '95, *Summaries of Papers Presented at the Conference on Lasers and Electro-Optics* Optical Society of America, Washington, DC, 1995, pp. 75,76.
[7] F.-Y. Tsai, C. P. Lee, J. Shen, Y. Oka, and H. H. Cheng, Microelectron. J. **30**, 367 (1999).
[8] S. Bar-Ad and I. Bar-Joseph, Phys. Rev. Lett. **68**, 349 (1992).
[9] A. Vinattieri, J. Shah, T. C. Damen, D. S. Kim, L. N. Pfeiffer, M. Z. Maialle, and L. J. Sham, Phys. Rev. B **50**, 10868 (1994).
[10] L. Munoz, E. Perez, V. Bellani, S. Zimmermann, L. Vina, K. Ploog, E. S. Koteles, and K. M. Lau, J. Opt. Soc. Am. B **13**, 994 (1996).
[11] V. Ciulin, G. Finkelstein, S. Haacke, J. D. Ganiere, V. Umansky, I. Bar-Joseph, and B. Deveaud, Physica B **256–258**, 466 (1998).
[12] M. C. Debnath, I. Souma, E. Shirado, H. Mitsu, T. Sato, J. X. Shen, and Y. Oka, J. Appl. Phys. **85**, 5941 (1999).
[13] L. V. Dao, M. Gal, G. Li, and C. Jagadish, J. Appl. Phys. **87**, 3896 (2000).
[14] S. L. Tyan, P. A. Shields, R. J. Nicholas, F.-Y. Tsai, and C. P. Lee, Jpn. J. Appl. Phys., Part 1 **39**, 3286 (2000).